THE JOURNAL OF PHYSICAL CHEMISTRY B

Article

pubs.acs.org/JPCB

Fickian Diffusion in Ternary Mixtures Composed by 1,2,3,4-Tetrahydronaphthalene, Isobutylbenzene, and *n*-Dodecane

V. Sechenyh,[†] J.C. Legros,[‡,§] A. Mialdun,[‡] J. M. Ortiz de Zárate,[∥] and V. Shevtsova[‡,*]

[†]Laboratoire de Physique, École Normale Supérieure, 46 Allé d'Italie, 69364 Lyon France

[‡]Microgravity Research Center, Université Libre de Bruxelles (ULB), CP-165/62, Av. F.D. Roosevelt, 50, B−1050 Brussels, Belgium

[§]National Research Tomsk Polytechnic University, Lenin Avenue, 30, 634050, Tomsk, Russia

[∥]Departamento de Física Aplicada I, Universidad Complutense de Madrid (UCM), Avda. de Séneca, 2 Ciudad Universitaria, 28040 Madrid, Spain

ABSTRACT: We report the Fickian diffusion coefficients in 20 ternary mixtures formed by 1,2,3,4-tetrahydronaphthalene (THN), isobutylbenzene (IBB) and *n*-dodecane (nC12) measured by the Taylor dispersion technique at 298.1 K and atmospheric pressure. Four diffusion coefficients of the ternary mixtures were measured along six concentration paths starting on one binary subsystem and moving toward the other one. We found expressions for the diffusion matrix of a ternary mixture approaching to the binary limits. The measured diffusion coefficients were thoroughly verified by comparison with the theoretical asymptotic behavior. The main diffusion coefficients vary smoothly over the entire concentration space and D_{11} is always larger than D_{22}. One of the two cross-diffusion coefficients is of the same order of magnitude as the main ones and, hence, not negligible, whereas the other one is close to zero. The investigated mixtures also comprise compositions that were examined in microgravity experiments in the ESA DCMIX$_1$ project.

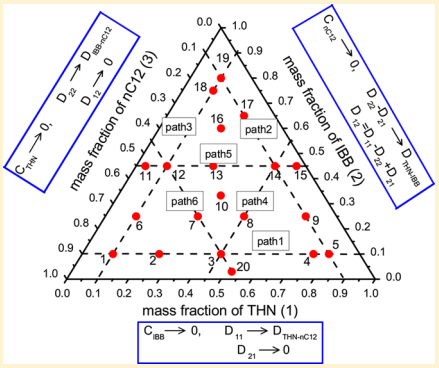

I. INTRODUCTION

Diffusion mass transfer commonly shows up in a number of industrial and ecological technologies and is important, especially, for a proper description of processes in chemical and petroleum engineering.[1] The latter application motivated active measurements of molecular diffusion in hydrocarbon liquid mixtures, particularly, in binary mixtures of alkanes.[2−4] The study of diffusion coefficients in multicomponent liquids which appear in nature and industrial applications is complicated due to several reasons. There is a lack of experimental values available even for the simplest case of a multicomponent mixture - ternary mixtures. A number of models and correlations[5,6] are built on empirical or semi-empirical grounds and, due to the limited amount of experimental data, their predictive capabilities are limited. Another example of theoretical models is based on the application of free volume/activation energy methods and molecular dynamics simulations. Recently published studies[7−10] allow to conclude that the above-mentioned models can be applied only inside a limited range of parameters.

Mainly due to experimental and mathematical difficulties, diffusion coefficients are so far available only for a limited number of ternary systems. Most commonly found in the literature are experimental data on mass diffusion in mixtures based on saturated and aromatic hydrocarbons or water solutions of simple and polyatomic alcohols with ketones. For example, diffusion coefficients in mixtures where all three components are hydrocarbons can be found only for two systems and limited to a few experimental points.[11−15] Fickian diffusion in mixtures of substances with associated molecules was discussed in the literature in more detail and is available for a few different ternary systems.[16−21]

The current interest in diffusion in multicomponent systems is also motivated by the DCMIX program (diffusion and thermodiffusion coefficients in mixtures) of the European Space Agency (ESA). Thermodiffusion effect (also called Soret, or thermal diffusion) is concentration separation in a liquid mixture as a response to the imposition of a thermal gradient. In the frame of this program the research groups conduct experiments on-board the International Space Station measuring thermodiffusion in binary[24] and ternary mixtures[25−28] to validate ground techniques. A recent benchmark study[29] has shown that unlike binary mixtures, the diffusion coefficients in ternary mixtures cannot be obtained from a thermodiffusion experiment with reliable accuracy and should be measured independently.

The description of the mass diffusion in ternary mixtures is significantly more complicated compared to binary mixtures. The diffusion coefficient is defined as the proportionality constant between a flux and a driving force. However, in ternary and higher mixtures the diffusion flux depends upon velocity reference frames: molar-, mass-, and volume-average velocity.[22]

Received: November 13, 2015
Revised: December 18, 2015
Published: December 23, 2015

DOI: 10.1021/acs.jpcb.5b11143
J. Phys. Chem. B 2016, 120, 535−548

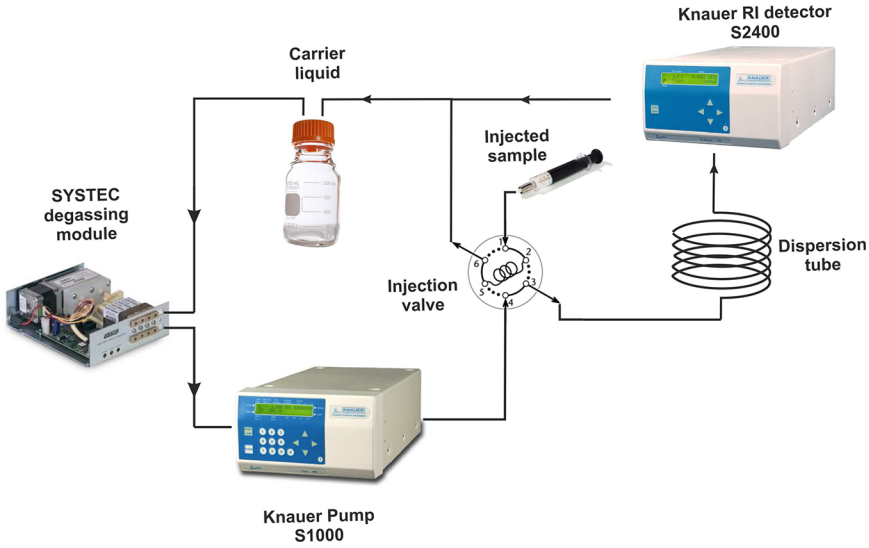

Figure 1. Schematic of the experimental setup. Flow direction is shown by arrows.

The mathematical model of the Taylor dispersion technique in ternary mixtures, utilized in the present study, was originally developed for the volume-average frame of reference.[23] Then the diffusive molar flux J_i of the component i is written as

$$J_i = -\sum_{j=1}^{N-1} D_{ij} \nabla C_j \quad (i = 1, ..., N-1) \tag{1}$$

where ∇C_j is the gradient of molar concentration of the component j and D_{ij} are the Fickian diffusion coefficients. The Fick description involves a matrix of diffusion coefficients $(N-1) \times (N-1)$ which is, generally, not symmetric, *i.e.*, $D_{ij} \neq D_{ji}$. The main diffusion coefficients D_{ii} connect the flux of the components i with its own concentration gradient, while the cross diffusivities D_{ij} describe the influence of the concentration gradient of the component j on the diffusive flux of the solute component i. With respect to a volume-fixed frame of reference the sum of fluxes is defined as $\sum J_i v_{im} = 0$, where v_{im} is the partial molar volumes of the i-component of a mixture.

A typical ternary mixture used by petroleum industry for reservoir modeling on the exploration stage is composed of 1,2,3,4-tetrahydronaphthalene (THN), isobutylbenzene (IBB) and *n*-dodecane (nC12), representing different families of molecules (polycyclic, aromatic, alkane). This mixture was also the first to be examined in convection free environment in the frame of the DCMIX$_1$ experiment.[25−28] Laboratory measurements by different techniques have been tested by comparing the results in a symmetric point of this mixture, i.e., the point with equal mass fractions.[11−14,30] Recently, the ternary diffusion coefficients were reported in four additional points.[13,29] The measurements of the different groups are in a good agreement only for eigenvalues of the diffusion matrix. In light of the experimental results available, it is desirable to analyze the evolution of the diffusion coefficients along the lines with constant concentration of one of the components and not in a single points. Here we present a comprehensive study of the Fickian diffusion coefficients THN−IBB−nC12 covering the entire concentration space using Taylor dispersion technique. The investigated compositions also comprise the five compositions that were examined in microgravity experiments in the ESA DCMIX$_1$ project.

The paper is organized as follows: Section II describes instrument, working equations, the details of the experimental procedure and preliminary analysis of obtained data. Section III includes analysis of the asymptotic behavior, variation of the diffusion coefficients along the concentration path and presents the concentration dependence of diffusion coefficients measured over a wide range of mixture compositions. Conclusions are given in section IV.

II. EXPERIMENTAL SECTION

A. Working Principle and Instrument. Among experimental methods developed for measurements of mass diffusion coefficients in liquids, the Taylor dispersion technique (TDT) has become standard for measuring coefficients in binary solutions[31] and lately has started to be extended to for three-component systems.[11,18,20,21,25,32] The TDT technique is based on the diffusive spreading of a small volume of a solution injected into a laminar stream of the same mixture but with a slightly different concentration. As the injected concentration pulse is carried through a tube, it is deformed by the coupled action of convection in the axial direction and molecular diffusion in the radial direction. At the end of the tube the shape of the pulse, sometimes called in the literature as the Taylor peak, is monitored by means of a suitable detector such as a flow-through spectrophotometer or a refractive index detector.

The principle scheme of the experimental setup used in this investigation is shown in Figure 1, while a detailed description was published previously.[11,12,25] The perturbing solution is injected at the entrance of a long dispersion tube with a circular cross-section made of polytetrafluoroethylene (PTFE). The inner diameter and length of the tube are $2R_0 = 748 \pm 1$ μm and $L = 29.839 \pm 0.001$ m, respectively. The inner radius R_0 was determined by gravimetry, i.e., from the mass of water required to fill the tube. The laminar flow of the carrier mixture is controlled by means of a pump Knauer Smartline S1000. In all the measurements, the flow rate was maintained constant 0.08 mL/min. The direction of the flow is shown by arrows in Figure 1. To prevent formation of bubbles, which spoil the quality of recorded signals, a SYSTEC degassing module was installed and connected in-line between the pump and a bottle with the carrier liquid. The concentration pulse was injected in

DOI: 10.1021/acs.jpcb.5b11143
J. Phys. Chem. B 2016, 120, 535−548

a stream of the carrier liquid with the help of 6-port/2-channel switching valve manufactured by Knauer GmbH. The injection valve was equipped with a 20 μL sampling tube and an electrical valve drive K-6 also manufactured by Knauer GmbH. The concentration as a function of time is monitored at the end of the dispersion tube by a differential refractive index detector (RID) Knauer Smartline RI 2400. The RID was equipped with a light source which works in the infrared spectrum (wavelength λ = 950 ± 30 nm). Typical values of the baseline noise were within the range $\pm 5 \times 10^{-8}$ V. The RID, the dispersion tube, and the pump were placed inside an air bath with a constant temperature of 298.1 ± 0.1 K. Activation of the electrical valve drive K-6 and automatic data acquisition were organized using the ClarityChrome chromatography software by DataApex.

B. Chemicals. All the measurements were performed with 1,2,3,4-tetrahydronaphthalene (THN), isobutylbenzene (IBB), and *n*-dodecane (nC12) without further purification. Short information about the chemical compounds used in the experiments is given in Table 1. Samples of mixtures with

Table 1. Sample Information

short name	source	mole fraction purity	analysis method	density, g/cm^3 (T = 298.15 K)	CAS number
THN	Acros Organics	0.98	GC[a]	0.973	119-64-2
IBB	Acros Organics	0.995	GC	0.850	538-93-2
nC12	Acros Organics	0.99	GC	0.753	112-40-3

[a]Gas−liquid chromatography.

different composition were prepared by weighing each component using electronic balances manufactured by Sartorius with resolution 0.1 mg/160g or 0.01g/4000g. Estimated error in mass fraction values is not more than ±0.0001.

C. Basic Equations of the TDT Technique. In the mathematical model it is assumed that a homogeneous liquid mixture flows through a long, isothermal, straight tube of length L with a uniform, circular cross-section of radius R_0, having impermeable walls. Alizadeh et al.[33] have shown that the coiling of the dispersion tube can be neglected under the following condition

$$De^2 Sc \leq 20 \tag{2}$$

where De and Sc are the Dean and Schmidt numbers, respectively:

$$\mathrm{Sc} = \frac{\mu}{\rho D}, \quad \mathrm{De} = \frac{2R_0 u\rho}{\eta\sqrt{R_{coil}/R_0}} \tag{3}$$

Here μ and ρ are the dynamic viscosity and density of a mixture; R_{coil} is the coil radius.

Further assumptions imply that diffusion coefficients are constant, which is valid if the concentration gradient is small, and no volume change occurs on mixing. The mixture is flowing in a slow, laminar manner with the mean velocity u. An injected narrow concentration pulse is dispersed due to the combined influence of the axial convection and molecular diffusion in the radial direction. The diffusion equation for each component can be written in the form:[23,33]

$$\frac{\partial C_i}{\partial t} = \sum_{j=1}^{2} D_{ij}\left(\frac{\partial^2 C_j}{\partial z^2} + \frac{\partial^2 C_j}{\partial r^2} + \frac{1}{r}\frac{\partial C_j}{\partial r}\right) - u\left[1 - 2\left(\frac{r}{R_0}\right)^2\right]\frac{\partial C_i}{\partial z} \quad (i, j = 1, 2) \tag{4}$$

here t is the time; r and z are the radial and axial coordinates, respectively.

It is considered that the axial transport by diffusion $\partial^2 C_j/\partial z^2 \ll \partial^2 C_j/\partial r^2 + r^{-1}\partial C_j/\partial r$ is small and can be neglected. In order to get an analytical solution of eq 4, an additional assumption is introduced: the time necessary to observe the effects of convective transport is long compared with the time in which the radial variations of concentrations are reduced by molecular diffusion to a fraction of their initial value. This condition was derived by Taylor[34] for a binary mixture (D is a binary diffusion coefficient):

$$\frac{L}{u} \gg \frac{R_0^2}{(7.22 \cdot D)} \tag{5}$$

Under these assumptions the radially averaged concentration of the injected sample can be written in the analytical form[33,36]

$$C(t) = C_0 + \frac{2\Delta C \Delta V}{R_0^3 u}\sqrt{\frac{3D}{\pi^3 t}}\exp\left(-\frac{12D(t - t_R)^2}{R_0^2 t}\right) \tag{6}$$

where $t_R = L/u$ is the retention time; ΔV is the volume of the injected solution sample; C is the mean concentration over the cross-section of a dispersion tube; C_0 is the concentration of a carrier solution; ΔC is a concentration difference between the injected sample and the carrier solution. For a practical implementation eq 6 was transformed by Leaist et al.[20,32] in order to replace the concentration C with the output signal of the RI detector

$$V(t) = \sum_{k=0}^{k=K} V_k t^k + \Delta V_{max}\sqrt{\frac{t_R}{t}}\exp\left(-\frac{12D(t - t_R)^2}{R_0^2 t}\right) \tag{7}$$

where V_k are the adjustable parameters of a baseline, usually it takes a polynomial form with K = 1 or 2, and ΔV_{max} is the peak height relative to the baseline.

Concentration differences ΔC must be sufficiently small to ensure that the changes in the detector signal $V(t)$ are proportional to the changes in the concentration across the dispersion profiles:

$$V(t) - \sum_{k=0}^{k=K} V_k t^k = R[C(t) - C_0] \tag{8}$$

where R = $\partial V/\partial C$ is the coefficient of proportionality, the so-called "detector sensitivity".

In the case of ternary mixtures, the equation for the detector signal includes two sensitivities $R_1 = (\partial V/\partial C_1)_{C_2}$ and $R_2 = (\partial V/\partial C_2)_{C_1}$:

$$V(t) = \sum_{k=0}^{k=K} V_k t^k + R_1[C_1(t) - C_{10}] + R_2[C_2(t) - C_{20}] \tag{9}$$

Here C_{10} and C_{20} are the concentrations in the carrier solution.

Following Leaist,[20,35] the analogue of eq 7 for a ternary mixture can be written as

DOI: 10.1021/acs.jpcb.5b11143
J. Phys. Chem. B 2016, 120, 535−548

$$V(t) = \sum_{k=0}^{k=K} V_k t^k + \Delta V_{max}\sqrt{\frac{t_R}{t}}\,[W_1 \exp(-\hat{D}_1\eta) + (1 - W_1)\exp(-\hat{D}_2\eta)] \quad (10)$$

where $\eta = 12(t - t_R)^2/R_0^2\, t$ and $\hat{D}_i$ are the eigenvalues of the matrix of diffusion coefficients:

$$\hat{D}_1 = \frac{1}{2}(D_{11} + D_{22} + \sqrt{(D_{11} - D_{22})^2 + 4D_{12}D_{21}}) \quad (11)$$

$$\hat{D}_2 = \frac{1}{2}(D_{11} + D_{22} - \sqrt{(D_{11} - D_{22})^2 + 4D_{12}D_{21}}) \quad (12)$$

Then the normalized weight W_1 is defined as

$$W_1 = \frac{(a + b\alpha)\sqrt{\hat{D}_2}}{(a + b\alpha)\sqrt{\hat{D}_1} + (1 - a - b\alpha)\sqrt{\hat{D}_2}} \quad (13)$$

where the parameters a, b and α are

$$a = \frac{D_{11} - \hat{D}_1 - \frac{R_1 D_{12}}{R_2}}{\hat{D}_2 - \hat{D}_1} \quad (14)$$

$$b = \frac{D_{22} - D_{11} - \frac{R_2 D_{21}}{R_1} + \frac{R_1 D_{12}}{R_2}}{\hat{D}_2 - \hat{D}_1} \quad (15)$$

$$\alpha = \frac{\Delta c_1}{\Delta c_1 + \left(\frac{\Delta c_2 M_1 R_1}{M_2 R_2}\right)} \quad (16)$$

Δc_1 and Δc_2 in eq 16 are the excess mass fractions in the injected solution; M_1 and M_2 are the molecular weights of mixture components. Equation 16 for α is already transformed from the molar concentrations C_i to our preferred concentrations in mass fraction $c_i = C_i M_i/\rho$, as discussed previously.[21]

Depending on the mixture, the eigenvalues $\hat{D}_i$ of a diffusion matrix could be distinct or equal. Hereafter we consider the case of distinct eigenvalues ($\hat{D}_1 \neq \hat{D}_2$). If the diffusion matrix is well conditioned, the eigenvalues as well as the coefficients a and b can be found by using the nonlinear least-squares technique to fit eq 10 to experimental profiles. Note that W_1 in eq 13 actually depends on the combination $a + b\alpha$, hence, to obtain independent values for a and b one has to fit two or more dispersion profiles simultaneously.[20,35] The criteria of the optimization during the fitting procedure can be a minimum of a residual function estimated as a sum of the squared differences between experimental and calculated values of a signal from the RI detector.

Equations 14-16 above depend on the ratio of detector sensitivities

$$S_R = \frac{R_1}{R_2} = \frac{\left(\frac{\partial V}{\partial C_1}\right)_{C_2}}{\left(\frac{\partial V}{\partial C_2}\right)_{C_1}} = \frac{M_1}{M_2}\frac{\left(\frac{\partial n}{\partial c_1}\right)_{c_2}}{\left(\frac{\partial n}{\partial c_2}\right)_{c_1}} \quad (17)$$

that, initially, can be determined from independent measurements of contrast factors at the wavelength of the refractometer. However, since available contrast factors[39] are for a slightly different wavelength, we also adopted here an alternative approach which evaluates S_R taking advantage of the fact that, for a ternary mixture, one has to perform at least two injections, each of them with different values of Δc_1 and Δc_2. Then, the ratio of detector sensitivities to concentration changes in the mixture can be measured in the course of Taylor experiment by[21]

$$S_R = \frac{R_1}{R_2} = \frac{M_1}{M_2}\frac{\Delta c_2^{(2)} S^{(1)} - \Delta c_2^{(1)} S^{(2)}}{\Delta c_1^{(1)} S^{(2)} - \Delta c_1^{(2)} S^{(1)}} \quad (18)$$

where $S^{(l)}$ is the surface area measured between dispersion profiles and baseline; the superscript (l) denotes the test number.

In case of distinct eigenvalues of the matrix D_{ik}, diffusion coefficients can be calculated from $\hat{D}_1$, $\hat{D}_2$, a, and b using the following equations:

$$D_{11} = \hat{D}_1 + \frac{a(1 - a - b)(\hat{D}_1 - \hat{D}_2)}{b} \quad (19)$$

$$D_{12} = \frac{a(1 - a)(\hat{D}_1 - \hat{D}_2)}{S_R b} \quad (20)$$

$$D_{21} = \frac{S_R(a + b)(1 - a - b)(\hat{D}_2 - \hat{D}_1)}{b} \quad (21)$$

$$D_{22} = \hat{D}_2 + \frac{a(1 - a - b)(\hat{D}_2 - \hat{D}_1)}{b} \quad (22)$$

A completely unconstrained four parameter fit may lead to nonphysical values of the main diagonal coefficients D_{ii} or the eigenvalues $\hat{D}_i$. The importance of establishing the proper restrictions was discussed previously by Mutoru and Firoozabadi[22] in the analysis of a large amount of diffusion data measured experimentally. The present study takes into account the restrictions for a multicomponent diffusion matrix which were outlined by Taylor and Krishna:[38]

$$D_{11} > 0,\ D_{22} > 0$$
$$D_{11}D_{22} - D_{12}D_{21} > 0$$
$$(D_{11} - D_{22})^2 + 4D_{12}D_{21} \geq 0 \quad (23)$$

D. Exploratory Measurements. Fickian diffusion coefficients have been measured in 20 ternary mixtures which are shown by the filled circles on the concentration map in Figure 2. In multicomponent mixtures values of diffusion coefficients depend on the numbering of the components.

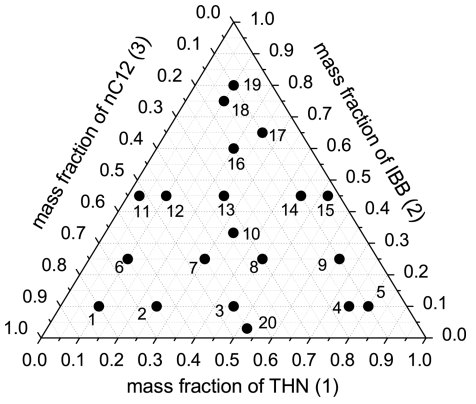

Figure 2. Circles show the concentrations in mass fractions at which the Fickian diffusion coefficients have been measured in the ternary mixture THN−IBB−nC12 (20 points).

DOI: 10.1021/acs.jpcb.5b11143
J. Phys. Chem. B 2016, 120, 535−548

Working with mixtures on a macroscopic scale, hydrodynamic effects become important. Thus, it is appropriate to choose the numbering of the component according to the density: THN (component 1), IBB (component 2), and nC12 (component 3). Consequently, two independent components are THN and IBB.

Another factor, which can influence the numbering of the components, is the sensitivity ratio S_R. The analytical equation used in the fitting procedure relies on the sensitivity ratio (see eqs 18 and 17). The diffusion coefficients cannot be measured with accuracy higher than the contrast factors $(\partial n/\partial c_i)_{c_j}$. The sensitivity ratio also depends on the order of the components. One should identify the large sensitivity ratio but escape the region when one of the contrast factors tends to zero (especially, the denominator). In order to determine the most favorable conditions for TDT measurements, the concentration dependence of the refractive index in ternary mixtures of THN−IBB−nC12 has been analyzed using the previous measurements by Sechenyh et al.[39] It appeared that the choice of THN and IBB as independent components also gives larger values of the sensitivity ratio S_R. It can be seen from the contour lines in Figure 3, that the sensitivity ratio S_R varies

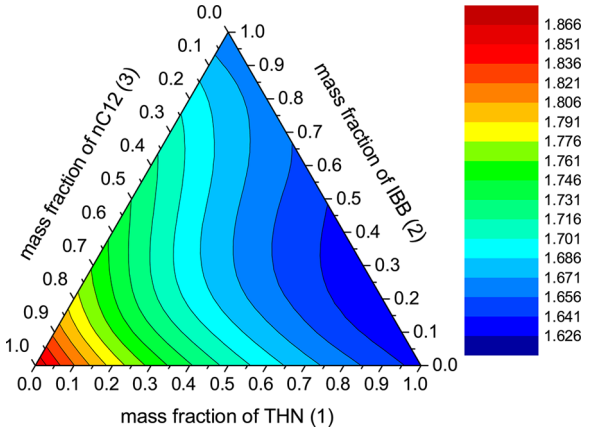

Figure 3. Concentration dependence of the sensitivity ratio $S_R = (\partial n/\partial c_1)_{c_2}/(\partial n/\partial c_2)_{c_1}$.

within ±6.9% over the full concentration space. The most favorable conditions for TDT measurements could be achieved in the concentration range when mass fractions of THN and nC12 are less than 0.2 and more than 0.9, respectively. As it was mentioned above, the sensitivity ratio S_R was also calculated using the surface areas between the measured dispersion profiles and the baseline (see eq 18) as in previously published works.[11,12,37]

One of the important practical points of the TDT technique is the choice of the appropriate flow rate for the carrier solution. The assumption made in the derivation of eqs 7 and 10 imposes constraints on the liquid velocity. The laminar flow of a carrier liquid should satisfy the condition mentioned in eq 5. Taking into account the literature values (by an order of magnitude) for diffusion coefficients, viscosity, density[11−15] and geometrical characteristics of the dispersion tube (see section IIA), eqs 5 can be satisfied only if the liquid velocity is $u < 0.16$m/s (flow rate less than 4.4 mL/min).

In order to select an optimal flow rate, tests have been performed with a carrier liquid with composition (0.52, 0.03, 0.45) and injected samples with composition (0.52, 0.06, 0.42). The ternary mixture was considered to be pseudobinary. Subsequently, the dispersion peak is characterized by a single diffusion coefficient, referred to as the pseudobinary diffusion coefficient D_{bin}. The coefficients D_{bin} were obtained by fitting the experimental points to the analytical solution derived for a case of the binary mixture, eq 7. Figure 4 shows the dependence

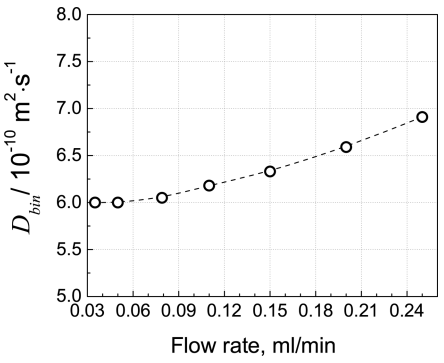

Figure 4. Dependence of the pseudobinary diffusion coefficient D_{bin} on the flow rate for the carrier mixture with composition (0.52, 0.03, 0.45) (point 20 in Figure 2).

of the pseudobinary diffusion coefficient D_{bin} as a function of the flow rate of the carrier liquid. It can be seen that a reasonable balance between the duration of experiments and the accuracy of measurements can be achieved if the flow rate is less than 0.1 mL/min ($u \leq 3.6 \times 10^{-3}$m/s). Another observation from Figure 4 is that the coefficient D_{bin} changes by 15% when the flow rate varies in the range between 0.03 and 0.25 mL/min. One of the explanations of such a significant dependence of the diffusion coefficient D_{bin} on the flow rate is the influence of the tube coiling discussed by Alizadeh et al.[33] In the present study, the flow rate was selected to be equal to 0.08 mL/min, which perfectly satisfies eq 2 and, at the same time, gives a reasonable duration of about 200−250 min for one single measurement.

To characterize the diffusion matrix at a particular concentration point c_{i0}, we have used a set of distinct samples $c_{i0} + \Delta c_i$. In practice it means that for the same composition of the carrier solution c_{i0} we have injected at least three samples with different Δc_i. The concentration differences Δc_i were chosen to be in the range ±0.04 g/g. Figure 5 shows the set of four injected samples that was used to determine the diffusion matrix for the mixture with composition (0.333, 0.333, 0.334).

It is worth noting that each sample was injected several times. The recorded peaks were subjected to thorough screening and the peaks which violated the repeatability of the pseudobinary diffusion coefficient or the predicted surface area were rejected. Then, the diffusion matrix was obtained from the simultaneous fit of all the selected peaks to the analytical model of the experiment.

The description of the algorithm for the extraction of the diffusion coefficients from the dispersion profiles was presented earlier.[11] The fitting of eq 10 to experimental signals was done by means of the iterative Nelder−Mead (simplex) algorithm[40] optimized for searching the minimum of a residual function in the space of four adjustable parameters: a, b, $\hat{D}_1$ and $\hat{D}_2$, see eqs 11, 12, 14 and 15. A sum of squared differences between experimental and calculated signals was chosen as a criterion of the iterative minimization procedure. Each solution was checked to satisfy the restrictions on the diffusion coefficients

DOI: 10.1021/acs.jpcb.5b11143
J. Phys. Chem. B 2016, 120, 535−548

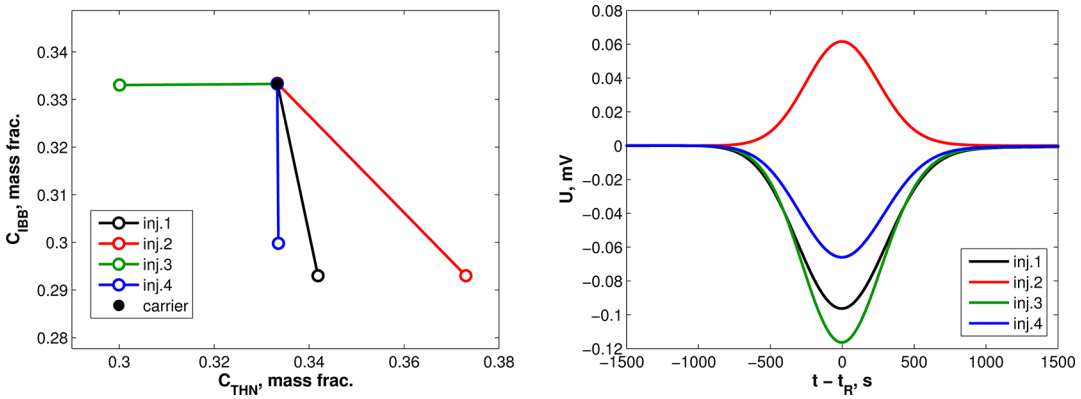

Figure 5. Set of samples used to determine the diffusion matrix in the mixture THN−IBB−nC12 with compositions in mass fractions (0.333, 0.333, 0.334): the left picture, carrier solution (filled circle) and injected samples (open circles) in the space of two independent concentrations; the right picture, dispersion peaks corresponding to the injections.

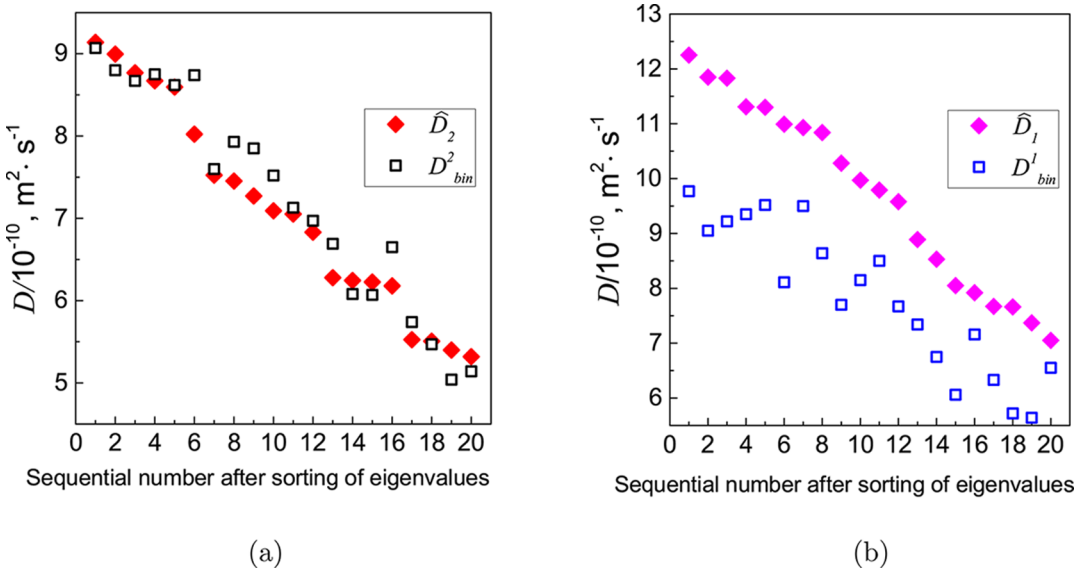

Figure 6. Comparison of the final eigenvalues of the diffusion matrix with the pseudobinary diffusion coefficients used as initial guesses for D_{11} and D_{22} (see text). The left picture: eigenvalue $\hat{D}_1$ with the $D_{bin}^{(1)}$ obtained from the injection with $\Delta c_2 = 0$. The The right picture: eigenvalue $\hat{D}_2$ with the $D_{bin}^{(2)}$ obtained from the injection with $\Delta c_1 = 0$. The horizontal axis is a sequential number over the all investigated mixtures, after sorting $\hat{D}_1$ from the largest to the smallest value.

mentioned above, i.e., eq 23. According to Mialdun et al.,[11] in the case of the ternary mixture THN−IBB−nC12, this iterative procedure with the simplex algorithm is almost insensitive to an initial guess (within a certain range of fitting parameters) and able to provide unambiguous results after 300−400 iterations. For all the investigated mixtures, the initial guesses of the iterative algorithm were chosen in a similar way: $D_{ij} = [D_{11}, D_{12}, D_{21}, D_{22}] = [D_{bin}^{(1)}, 0, 0, D_{bin}^{(2)}]$, where the pseudobinary diffusion coefficients $D_{bin}^{(1)}$ and $D_{bin}^{(2)}$ are obtained from ternary dispersion profiles corresponding to injections of solutions with $\Delta c_2 = 0$ and $\Delta c_1 = 0$, respectively (i.e., injections 3 and 4 for the example of Figure 5). Direct comparison of the initial $D_{bin}^{(1)}$ and $D_{bin}^{(2)}$ with the final results of the fitting leads us to the conclusion that the proposed initial guesses can be used in a wide range of mixture compositions. Furthermore, these pseudobinary diffusion coefficients display some common features with the finally obtained eigenvalues, as shown in Figure 6a, which demonstrates that the values of $D_{bin}^{(2)}$ are similar to those finally obtained for $\hat{D}_2$. The final eigenvalue $\hat{D}_1$ is always larger than $D_{bin}^{(1)}$, but the difference is not very significant, as seen in Figure 6b. A similar correspondence between pseudobinary diffusion coefficients and finally obtained eigenvalues was also observed in the ternary mixture water−ethanol−triethylene glycol.[21]

Before concluding this section, we should mention that the theory of TDT assumes no volume changes and that the density of the injected samples is the same as that of the carrier liquid. This allows us to assume that mass density does not depend on composition, and in that case, the diffusion matrix is the same in the volume and in the mass reference frame. In addition, since the molecular weights of the three components of our mixture are quite similar, the diffusion matrix will be approximately the same also in the molar frame of reference.

III. RESULTS AND DISCUSSION

A. Behavior of Ternary Diffusion Coefficients Approaching Binary Limits. The TDT allows to obtain four diffusion coefficients from the experiments, however, there are several potential pitfalls. One of them is that a minimized residual function may take the form of a deep and long valley in

DOI: 10.1021/acs.jpcb.5b11143
J. Phys. Chem. B 2016, 120, 535−548

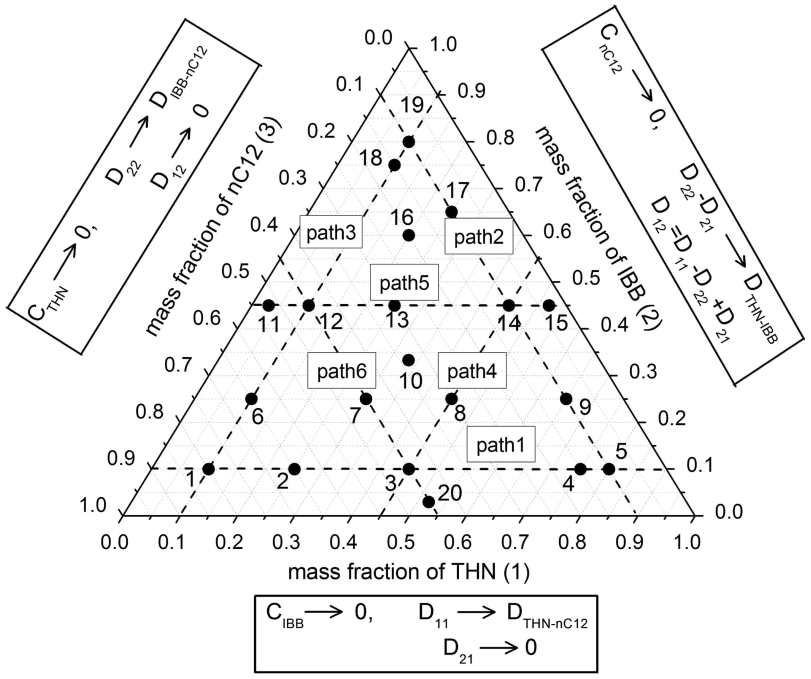

Figure 7. Concentration paths and asymptotic behavior of the diffusion matrix D_{ij} close to the boundaries of the concentration triangle. Each path corresponds to one constant concentration among the three components. Three concentration paths correspond to $c_i = 0.1$, and the other three paths correspond to $c_i = 0.45$.

a parameter space that leads to a large uncertainty. Particularly for this ternary mixture THN−IBB−C12, previous studies in the symmetric point with compositions in mass fractions (0.333, 0.333, 0.334) have demonstrated that such a problem is present.[11,41] Therefore, an independent quality control of the obtained solutions is a real necessity for ternary mixtures. The behavior of ternary diffusion coefficients when approaching the binary limits provides an efficient way for the validation of the experimental results.

The measurements of binary diffusion coefficients are generically more accurate and reliable than the measurements of ternary diffusion matrices, mainly due to the absence of the cross-diffusion phenomenon. In addition, databases of binary diffusion coefficients are usually more exhaustive and complete compared to the few experimental data available for ternary diffusion matrices. Several authors[42,43] have discussed the asymptotic behavior of the diffusion matrices and their eigenvalues and eigenvectors close to the boundaries of the concentration triangle. Here we present a simple and convenient way to obtain these limits based on the consideration of the mass diffusion fluxes, in which case these conditions are more readily expressed. Since diffusion coefficients obtained from the TDT are equal for both the volume and the mass reference frames, these asymptotic limits should apply to our experimental results. The two independent mass fluxes in a ternary mixture can be written as

$$-j_1/\rho = D_{11}\nabla c_1 + D_{12}\nabla c_2 \tag{24}$$

$$-j_2/\rho = D_{21}\nabla c_1 + D_{22}\nabla c_2 \tag{25}$$

When approaching the binary mixture THN-nC12 at the bottom of the triangle in Figure 7, the IBB content (c_2) tends to zero as well as its mass flux, i.e., $\nabla c_2 \to 0$ and $j_2 \to 0$. Then from eq 25 it follows that $D_{21} \to 0$, and from eq 24, it follows that $D_{11} \to D_{\text{bin}}^{\text{THN-nC12}}$, where $D_{\text{bin}}^{\text{THN-nC12}}$ is the diffusion coefficient measured in a binary mixture of THN and nC12 at the corresponding concentration. Note that the behavior of D_{22} and D_{12} in this limit cannot be predicted from this analysis.

On the left-hand side of the triangle, the concentration of THN (c_1) and its mass flux j_1 vanish, i.e., $\nabla c_1 \to 0$ and $j_1 \to 0$. Consequently, from eq 24 it follows that $D_{12} \to 0$ and from eq 25 follows that $D_{22} \to D_{\text{bin}}^{\text{IBB-nC12}}$, where $D_{\text{bin}}^{\text{IBB-nC12}}$ is the diffusion coefficient measured in a binary mixture of IBB and nC12 at the corresponding concentration. Again, the behavior of the two other coefficients, D_{11} and D_{21}, in this limit cannot be predicted from this analysis.

On the right-hand side of the triangle the concentration of nC12 (c_3) and its mass flux j_3 vanish. The mass flux for the third component $j_3 = -j_1 - j_2$ can be written as

$$j_3/\rho = (D_{11} + D_{21})\nabla c_1 + (D_{12} + D_{22})\nabla c_2 \tag{26}$$

Selecting the concentration of the second and third components as independent variables, from the condition $c_1 + c_2 + c_3 = 1$, it follows that $\nabla c_1 = -(\nabla c_2 + \nabla c_3)$ and the expressions for the mass fluxes j_2 and j_3 take form

$$-j_2/\rho = (D_{22} - D_{21})\nabla c_2 - D_{21}\nabla c_3 \tag{27}$$

$$j_3/\rho = -(D_{11} + D_{21} - D_{12} - D_{22})\nabla c_2 - (D_{11} + D_{21})\nabla c_3 \tag{28}$$

Applying the same logic as above, from the conditions $\nabla c_3 \to 0$ and $j_3 \to 0$ and eq 28, it follows that $D_{11} + D_{21} - D_{12} - D_{22} = 0$, while from eq 27, it follows that $(D_{22} - D_{21}) \to D_{\text{bin}}^{\text{THN-IBB}}$. This set of asymptotics is summarized graphically in Figure 7 over the concentration triangle of the THN-IBB-C12 mixture. They can also be summarized in the following expression:

DOI: 10.1021/acs.jpcb.5b11143
J. Phys. Chem. B 2016, 120, 535−548

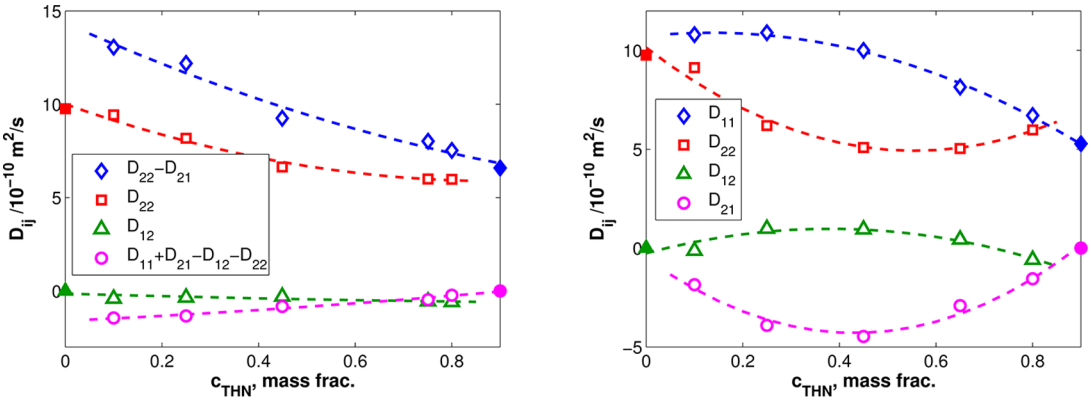

(a) Path 1: C_{IBB}=0.1

(b) Path 2: C_{nC12}=0.1

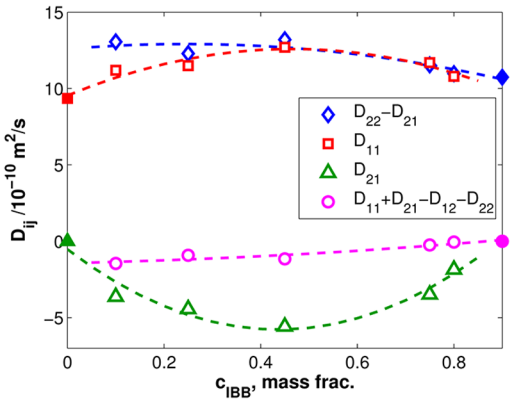

(c) Path 3: C_{THN}=0.1

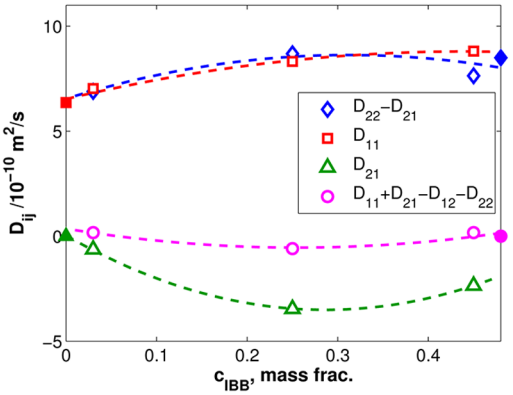

(d) Path 4: C_{THN}=0.45

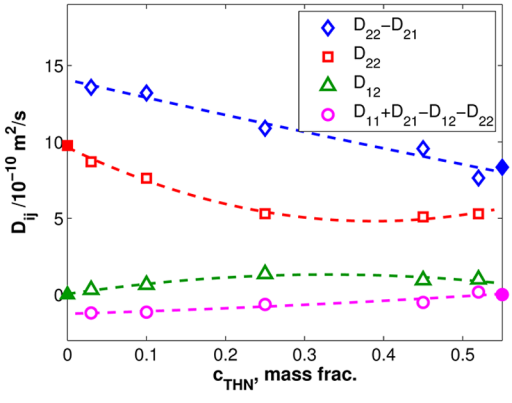

(e) Path 5: C_{IBB}=0.45

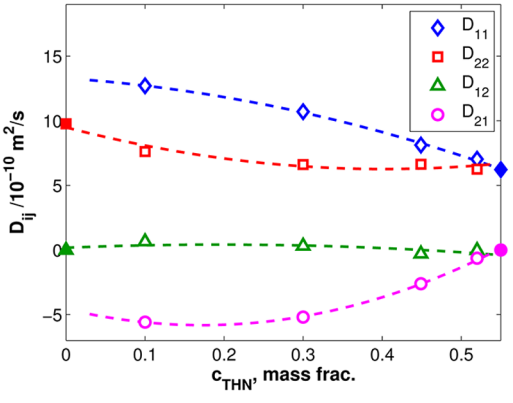

(f) Path 6: C_{nC12}=0.45

Figure 8. Combination of Fickian diffusion coefficients D_{ij} having well-defined binary limits (see eq 29) along concentration paths in the ternary system THN-IBB-C12. One of the concentrations on each path is constant as written on the panels. The filled symbols indicate asymptotic values approaching the binary subsystems. The dotted trend lines are given as guidance for the eyes.

DOI: 10.1021/acs.jpcb.5b11143
J. Phys. Chem. B 2016, 120, 535−548

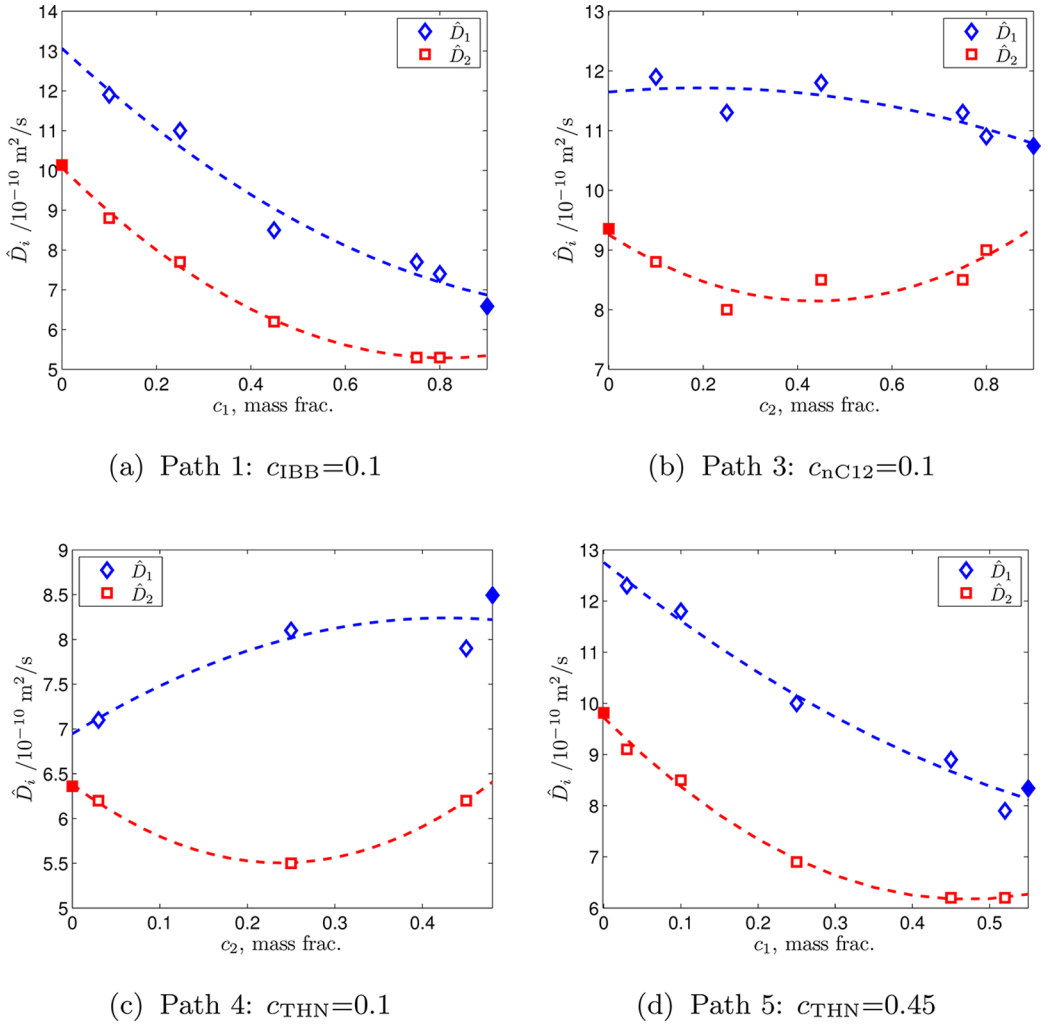

(a) Path 1: c_{IBB}=0.1 (b) Path 3: c_{nC12}=0.1

(c) Path 4: c_{THN}=0.1 (d) Path 5: c_{THN}=0.45

Figure 9. Eigenvalues of Fickian diffusion coefficients $\hat{D}_i$ along some of the concentration paths in the ternary system THN−IBB−nC12 shown in Figure 8. The filled symbols indicate asymptotic values approaching the binary subsystems according to eq 30. The dotted trend lines are given as the guidance for the eyes.

$$\text{when } c_1 \to 0: \quad \begin{cases} D_{22} \to D_{\mathrm{bin}}^{(23)}, \\ D_{12} \to 0, \end{cases}$$

$$\text{when } c_2 \to 0: \quad \begin{cases} D_{11} \to D_{\mathrm{bin}}^{(13)}, \\ D_{21} \to 0, \end{cases}$$

$$\text{when } c_3 \to 0: \quad \begin{cases} (D_{22} - D_{21}) \to D_{\mathrm{bin}}^{(12)}, \\ D_{11} + D_{21} - D_{12} - D_{22} \to 0, \end{cases} \tag{29}$$

where, again, $D_{\mathrm{bin}}^{(ij)}$ represents the diffusion coefficient that is measured in a *binary* mixture of components i and j. In conclusion, when approaching the boundaries of the concentration triangle in a ternary mixture, one of the main diagonal coefficients of the diffusion matrix tends to the binary diffusion coefficient on two sides of the triangle. At the same time, at least one of the cross-diagonal coefficients of the diffusion matrix tends to zero on these same sides.

It is also interesting to study the binary limits of the two eigenvalues of the diffusion matrix, that can be easily inferred by combining eqs 11 and 12 with eq 29. It can be shown that at each side of the concentration triangle, one of the eigenvalues is determined by the corresponding binary diffusion coefficient. For the particular mixture we consider here $D_{11} > D_{22}$ over the whole concentration range except for $c_2 \to 0$ (see a more complete discussion below), while $D_{12} + D_{21} < 0$ everywhere, in particular over the $c_3 = 0$ axis. From these conditions, some algebra leads one to conclude:

$$\begin{aligned} &\text{when } c_1 \to 0: \quad \hat{D}_2 \to D_{\mathrm{bin}}^{(23)}, \\ &\text{when } c_2 \to 0: \quad \hat{D}_2 \to D_{\mathrm{bin}}^{(13)}, \\ &\text{when } c_3 \to 0: \quad \hat{D}_1 \to D_{\mathrm{bin}}^{(12)}. \end{aligned} \tag{30}$$

In a more general case, due to the nonlinear structure of eqs 11 and 12 which one of the eigenvalues can be constrained at each side of the concentration triangle depends on the magnitude of D_{ij}.

B. Diffusion Coefficients along Concentration Paths.

We proceed now with the analysis of the diffusion coefficients in the ternary mixture THN-IBB-C12 obtained by the Taylor dispersion technique. The measured points were organized in six concentration paths presented in Figure 7; each of them started on a binary subsystem and continued along the line with a constant concentration of one of the components toward another binary subsystem. Along each path one of the

DOI: 10.1021/acs.jpcb.5b11143
J. Phys. Chem. B 2016, 120, 535−548

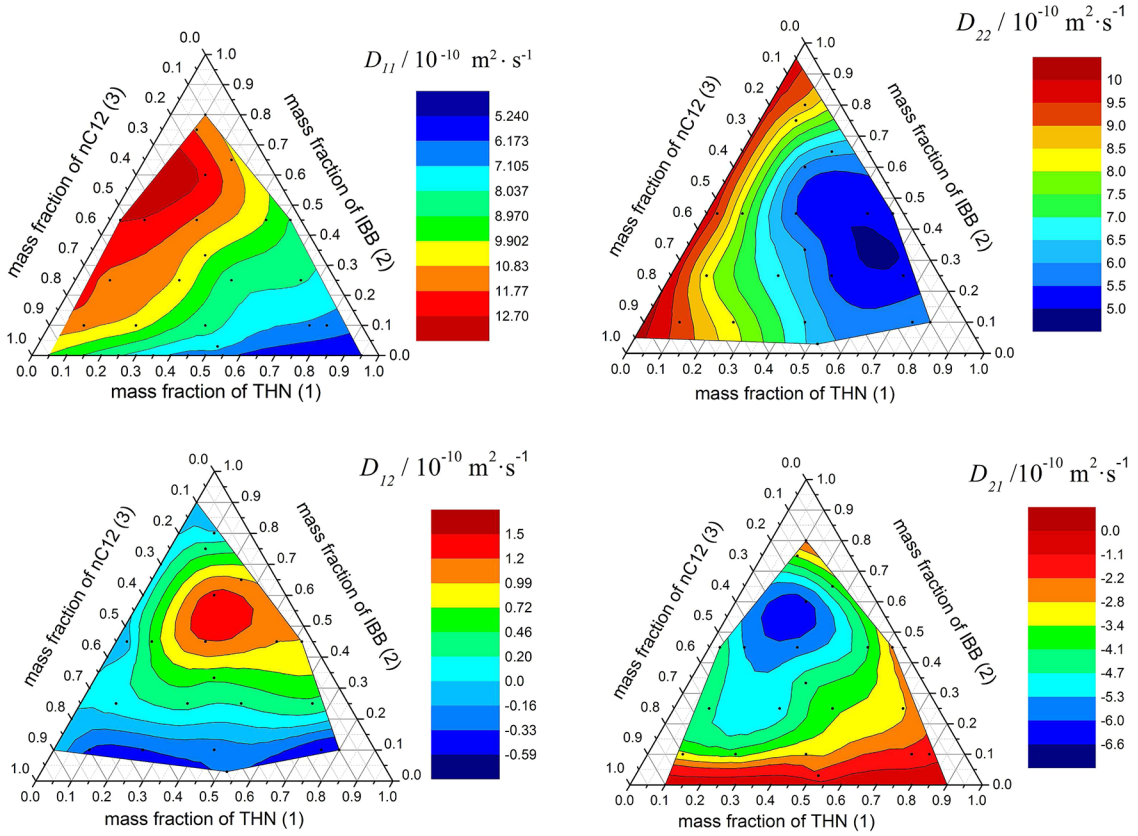

Figure 10. Fickian diffusion coefficients D_{ij} over measured concentration space in the ternary system THN−IBB−nC12. The concentration is expressed in mass fraction units. Color scales indicate the variation amplitude of the quantities. Small dots indicate experimental points.

Table 2. Compositions of Ternary Mixtures THN(1) + IBB(2) + nC12(3) in Mass Fractions, Diffusion Coefficients $D_{ij}/10^{-10}$ m^2/s, Eigenvalues of the Diffusion Matrix $\hat{D}_i/10^{-10}$ m^2/s, and Determinant of the Diffusion Matrix $Det/10^{-19}$ m^4/s^2 [a]

point	c_1	c_2	c_3	D_{11}	D_{12}	D_{21}	D_{22}	$\hat{D}_1$	$\hat{D}_2$	det
1	0.100	0.100	0.800	11.2	−0.41	−3.63	9.43	11.9	8.8	10.4
2	0.250	0.100	0.650	10.5	−0.35	−4.01	8.18	11.0	7.7	8.44
3	0.449	0.102	0.449	8.12	−0.30	−2.61	6.64	8.5	6.2	5.31
4	0.751	0.101	0.148	6.99	−0.56	−2.02	6.00	7.7	5.3	4.08
5	0.800	0.100	0.100	6.71	−0.59	−1.55	5.98	7.4	5.3	3.92
6	0.100	0.250	0.650	11.5	0.13	−4.44	7.85	11.3	8.0	9.07
7	0.300	0.250	0.450	10.7	0.31	−5.19	6.61	10.3	7.1	7.25
8	0.500	0.250	0.250	8.32	0.22	−3.46	5.23	8.1	5.5	4.43
9	0.650	0.250	0.100	8.15	0.44	−2.91	5.04	7.7	5.5	4.24
10	0.333	0.333	0.334	10.1	0.40	−4.07	6.33	9.6	6.8	6.55
11	0.030	0.450	0.520	12.7	0.32	−4.88	8.70	12.3	9.1	11.2
12	0.100	0.450	0.450	12.7	0.65	−5.58	7.62	11.8	8.5	10.0
13	0.250	0.450	0.300	11.6	1.35	−5.59	5.30	10	6.9	6.89
14	0.450	0.450	0.100	10.0	0.95	−4.47	5.09	8.9	6.2	5.52
15	0.520	0.450	0.030	8.81	1.00	−2.35	5.29	7.9	6.2	4.89
16	0.200	0.600	0.200	12.7	1.46	−6.48	5.63	10.8	7.5	8.07
17	0.250	0.650	0.100	10.9	0.98	−3.91	6.20	9.8	7.3	7.12
18	0.100	0.750	0.150	11.7	0.39	−3.48	8.07	11.3	8.5	9.59
19	0.100	0.800	0.100	10.8	−0.13	−1.85	9.13	10.9	9.0	9.83
20	0.520	0.030	0.450	7.03	−0.03	−0.63	6.26	7.1	6.2	4.40

[a]The first column indicates the point number in Figure 2 and Figure 7. All reported data are for the temperature T = 298.1 K.

concentrations is kept constant; three paths correspond to c_i = 0.1 and other three paths corresponds to c_i = 0.45. The points on two paths (5 and 6) very closely approach to binary limits in order to trace accurately the asymptotic behavior. For each concentration path we present in Figure 8 four combinations of D_{ij} which has well-defined binary limits, as summarized in eq 29. The filled symbol of the same type as the open ones indicates the asymptotic value of the coefficient near the binary limit. Data for the diffusion coefficients of the three binary subsystems have been taken from Gebhardt et al.[44]

DOI: 10.1021/acs.jpcb.5b11143
J. Phys. Chem. B 2016, 120, 535−548

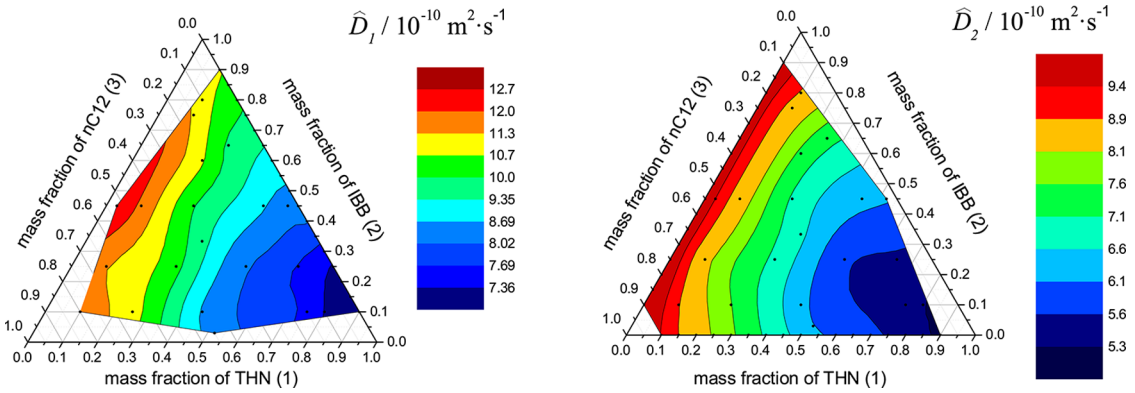

Figure 11. Concentration dependence of the eigenvalues of the diffusion matrix D_{ij}.

The first observation is that, for all the concentration paths analyzed, our measurements perfectly meet the expectations at the binary limits. Indeed, as seen in Figure 8 on panels a, c, d, and e, the values $(D_{11} + D_{21} - D_{12} - D_{22})$ smoothly tend to zero and $(D_{22} - D_{21})$ tend to $D_{\mathrm{THN-IBB}}$ when the ternary system approaches, by different concentration paths, the right-hand side of the triangle. It worth noting that the quantity $(D_{11} + D_{21} - D_{12} - D_{22})$ is very close to zero along all the four presented paths. The main diagonal coefficients are consistent with the corresponding binary limits given by eq 29. From the different panels of Figure 8 one further observes that the numerical value of the cross-diffusion D_{12} is always very small, while the other cross-diffusion D_{21} is always negative, non-negligible in general, but it rapidly approaches zero when the concentration of IBB (c_2) does, see panels (a) and (b). The positive outcome in the discussion of the binary limits gives confidence that both the experimental approach and fitting procedure provide valid results.

To complete the discussion of binary limits, we show in Figure 9 the eigenvalues of Fickian diffusion coefficients $\hat{D}_i$ along some of the concentration paths in the ternary system THN−IBB−nC12 shown in Figure 8. The asymototic limits given by eq 30 have been added to the figure as filled symbols, taken from the data published by Gebhardt et al.[44] One observes in Figure 9 that in all cases the measured eigenvalues smoothly approaches the expected binary limits as given by eq 30, adding further confirmation to the D_{ij} values measured in the present work.

C. Summary and Comparison of the Experimental Results. The four Fickian diffusion coefficients measured in the present work for the ternary system THN−IBB−nC12 are presented graphically as contour maps in Figure 10, demonstrating the concentration dependence of the main and cross-diagonal coefficients of the diffusion matrix. Notice that the color scale at each triangle is different because the variation amplitude of each quantity is different. The asymptotic behavior near binary limits given by eq 29, has been incorporated into the plots of Figure 10, taking the data for the binary subsystems from from Gebhardt et al.[44] As it is seen in Figure 10, both main diagonal coefficients D_{11} and D_{22} exhibit distinct nonlinear behavior, with extreme points in different parts of the component concentration triangle. In particular, coefficient D_{11} reaches its maximum value in THN poor region of the triangle, i.e., in the range of mixture compositions where $c_1 \leq 0.2$ and $0.5 \leq c_2 \leq 0.7$. Coefficient D_{22} exhibits a minimum in nC12 poor region of the triangle, when $0.5 \leq c_1 \leq 0.7$ and $0.3 \leq c_2 \leq 0.4$. It should be mentioned that, for all 20 investigated mixtures, D_{11} is larger than D_{22} (see Table 2) although the difference decreases as $c_2 \rightarrow 0$ and, actually, for the point closer to the $c_2 = 0$ axis (no. 20 in Table 2), both coefficients are identical within experimental errors. As can be further observed in Figure 10, the magnitude (absolute value) of D_{12} is smaller than D_{21} over the whole composition range. These off-diagonal coefficients of the diffusion matrix, D_{12} and D_{21}, exhibit as a function of the concentrations visible regions of extremum. The coefficient D_{12} has a maximum when $0.15 \leq c_1 \leq 0.35$ and $0.45 \leq c_2 \leq 0.65$. Minimum values of D_{21} are observed when $0.1 \leq c_1 \leq 0.3$ and $0.5 \leq c_2 \leq 0.65$. In the concentration triangle of Figure 10c one can observe a region where the coefficient D_{12} changes sign from positive to negative values. However, D_{12} has a negative sign throughout the area of the concentration triangle of Figure 10d. Over the entire concentration space the system does not reveal a sharp change of the coefficients.

Contour maps for the eigenvalues $\hat{D}_1$ and $\hat{D}_2$ are presented in Figure 11, showing a smooth and gradual change in the magnitude of both. Minimum values of $\hat{D}_1$ and $\hat{D}_2$ are observed in the region where the mass fraction of THN is larger than 0.7, while maximum eigenvalues are shown when ternary mixture contains small quantities of THN (less than 0.1).

The numerical values of the data shown in Figures 10 and 11 are listed in Table 2, containing quantitative results for the diffusion coefficients measured by Taylor dispersion in the ternary mixture THN−IBB−nC12. The table presents the four diffusion coefficients, the eigenvalues and the determinant of the diffusion matrix for all the investigated mixture compositions shown in Figure 2.

As it was mentioned in the Introduction, the ternary mixture of THN−IBB−nC12 has been studied as a benchmark solution. Table 3 presents data available in the literature for the diffusion coefficients measured by different experimental techniques: sliding symmetric tubes,[13,29] optical beam deflection technique,[14] counter flow cell technique[15] and open-ended capillary technique.[26] Note that, for all the listed data in Table 3, the eigenvalues were recalculated according to eqs 11 and 12. Direct comparison of Tables 2 and 3 is possible only for the experimental points labeled in Figure 2 by numbers 1, 5, 10, 19. Particularly interesting comparisons can be made for the two points no. 5 (0.8, 0.1) and no. 10 (0.33, 0.33) where the results of more than two sources can be balanced. The first observation is that all techniques in these two points provide somewhat similar eigenvalues, although with some apparent discrepancies.

DOI: 10.1021/acs.jpcb.5b11143
J. Phys. Chem. B 2016, 120, 535−548

Table 3. Comparison of Ternary Diffusion Coefficients Measured in Mixtures of THN(1)−IBB(2)−nC12(3) by Different Experimental Techniques[a]

c_1	c_2	D_{11}	D_{12}	D_{21}	D_{22}	$\hat{D}_1$	$\hat{D}_2$
Sliding Symmetric Tubes (SST)[13,29]							
0.10	0.10	10.00	−0.8	−1.5	10.00	11.1	8.9
0.45	0.10	7.15[b]	0.32	−0.14	6.63[b]	7.04	6.74
0.40	0.20	8.00	1.3	−1.3	4.00	7.5	4.5
0.10	0.80	10.00	−0.21	−1.7	7.00	10.1	6.9
0.33	0.33	8.00	−2.30	−2.00	6.00	9.4	4.6
0.80	0.10	5.2	−1.1	0.4	8.3	8.2	5.4
Optical Beam Deflection Technique (OBD)[14]							
0.33	0.33	5.62	−5.91	1.08	12.18	10.99	6.81
Counter Flow Cell Technique (CFC)[15]							
0.33	0.33	11.6	0.32	−6.18	6.65	11.2	7.09
Open-Ended Capillary Technique (OEC)[26]							
0.80	0.10	5.5	−0.99	0.002	6.6	6.6	5.5

[a]The first two columns indicate concentrations c_i in mass fractions and then diffusion coefficients $D_{ij}/10^{-10}$ m^2/s and eigenvalues $\hat{D}_i/10^{-10}$ m^2/s. [b]Private communication.

The main issue which rises up from the comparison of Tables 2 and 3 is related to the main diffusion coefficients: which of them is larger, D_{11} or D_{22}? One can analyze this issue in more detail referring to previous measurements of diffusion coefficients in the binary subsystems.[44] From these measurements and the correlations therein one can estimate the diffusion coefficients of THN and IBB at the infinite dilution limits and, thus, obtain a rough idea on the ratio of their mobilities within the ternary media. Diffusion coefficients of THN at infinite dilution in IBB and nC12 are $D^{\infty}_{\mathrm{THN-IBB}} = 11.3 \times 10^{-10}$ m^2/s and $D^{\infty}_{\mathrm{THN-nC12}} = 10.4 \times 10^{-10}$ m^2/s, respectively. Isobutylbenzene at infinite dilution limit in tetralin and *n*-dodecane has diffusion coefficients $D^{\infty}_{\mathrm{IBB-THN}} = 6.1 \times 10^{-10}$ m^2/s and $D^{\infty}_{\mathrm{IBB-nC12}} = 10.3 \times 10^{-10}$ m^2/s, respectively. Then, one may expect that in mixed media tetralin will have somewhat larger mobility with respect to isobutylbenzene, and so, superiority of D_{11} over D_{22} is expected. This is in line with our experimental observations, where D_{11} is always larger than D_{22}. However, notice that approaching to the bottom side when $c_2 \to 0$ the difference $(D_{11} - D_{22})$ diminishes; see in Table 2 the points labeled nos. 4, 5, and 20. This last observation can lead to consistency with both the measurements by SST[13,29] and OEC[26] which report $D_{22} > D_{11}$ for small concentration of IBB.

Note that the investigated mixtures also comprise four compositions that were examined in microgravity experiments in the ESA DCMIX$_1$ project, they are labeled in Figure 2 by nos. 1, 5, 14, and 19. The fifth DCMIX$_1$ point (0.40, 0.20, 0.40) is out of the selected paths, but the diffusion coefficients can be easily evaluated from the values on path nos. 4 and 6. The measured diffusion coefficients will provide a valuable support for obtaining Soret coefficients from DCMIX$_1$ raw data.

An important remaining question from the studies carried out in this work is correct evaluation of experimental uncertainties. All experimental data have associated uncertainties, no matter how hard one tries to minimize them. In multicomponent diffusion measurements the problem of uncertainty is really tough due to several reasons. First, the diffusion coefficients are obtained by fitting (solution of a minimization problem) and not by straightforward calculations. Second, an objective function subjected to the minimization possesses a pronounced valley-type landscape.[11] These features lead to high sensitivity of the results to small experimental imperfections and to extended scattering of measured coefficients.

The experimental uncertainty was evaluated in the following way. Determination of full diffusion matrix relies on several (by default $n = 3$) samples and each of them was injected several times (by default $k = 3$ as well). Three data sets were used simultaneously in the fitting procedure. Since the injection of each of the three samples was repeated three times, the number of possible permutations forming a cluster of three data sets is $k^n = 27$. Each data set was subjected to fitting as an individual experiment. With such an approach, by conducting $n \times k = 9$ experimental runs, we obtained 27 sets of sought coefficients for the same diffusion experiment. Then the average values and standard deviations were calculated. One may also express the relative uncertainty (in percents), when the standard deviation is divided by the average value. The calculated relative uncertainty yielded coherent results which can be applied to all measurements:

$$\sigma_{D_{11}} = 2\%,\ \sigma_{D_{21}} = 8\%,\ \sigma_{D_{22}} = 4\%$$

$$\sigma_{\hat{D}_1} = 3\%,\ \sigma_{\hat{D}_2} = 1.5\%$$

We do not provide a relative uncertainty of the coefficint D_{12} whose numerical value is very close to zero. The smallest error is attributed to the minor eigenvalue. It is expected, because namely the minor eigenvalue dominates in the majority of experimental signals, as can be seen, *e.g.*, in Figure 6. The presented combinatorial approach was used only for the error estimation in several points. For the regular results processing, the simultaneous fit of the full data set consisting of $n \times k = 9$ runs was used as it is less labor intensive.

IV. CONCLUSIONS

We have performed a comprehensive study of the Fickian diffusion coefficients in the ternary liquid mixture of 1,2,3,4-tetrahydronaphthalene (THN, **1**), isobutylbenzene (IBB, **2**) and *n*-dodecane (nC12, **3**) at a constant temperature of $T = 298.1$ K and at atmospheric pressure. The mutual diffusion coefficients were measured in 20 compositions of mixtures by using the Taylor dispersion technique. It was found that the off-diagonal elements of the diffusion matrix cannot be neglected for this ternary mixture of hydrocarbons. In particular, the numerical value of the cross-diffusion D_{21} has almost the same order of magnitude as the main diffusion coefficient D_{22}, but a negative one. The other cross diffusion coefficient, D_{12}, is always very small. A similar disparity between off-diagonal elements was observed in the associated ternary mixture of water−ethanol−triethylene glycol.[21] The main diffusion coefficients are positive and vary smoothly over the entire concentration space in the range of $(5.0-12.7) \times 10^{-10}$ m^2/s. The main diffusion coefficient D_{11} is always larger than the other one, $D_{11} > D_{22}$.

Which of the main diffusion coefficients is larger has been an open question in the current literature,[13−15,26] which seems to be closed by this work. The advantage of the present study is that coefficients were measured not in a single point but along concentration paths starting on one binary subsystem and moving toward to other one. First, we derived expressions for the asymptotic behavior of a ternary mixture approaching binary limits. Then, on each of six concentration paths, we presented rigorous evidence that the constrains at the binary

DOI: 10.1021/acs.jpcb.5b11143
J. Phys. Chem. B 2016, 120, 535−548

limits are perfectly fulfilled. Such a positive outcome gives confidence that both the experimental approach and the fitting procedure provide valid results. We hope that the present experimental results will motivate new diffusion research, in particular, molecular dynamic simulations.

AUTHOR INFORMATION

Corresponding Author

*(V.S.) E-mail: vshev@ulb.ac.be.

Notes

The authors declare no competing financial interest.

ACKNOWLEDGMENTS

This work is funded by the FNRS (Fonds de la Recherche Scientifique) foundation and also supported by the PRODEX programme of the Belgian Federal Science Policy Office, ESA. Research at UCM is partly funded by the Spanish State Secretary of Research under Grant No. FIS2014-58950-C2-2-P.

REFERENCES

(1) Shapiro, A. A.; Davis, P. K.; Duda, J. L. Diffusion in Multicomponent Mixtures; In *Computer Aided Property Estimation*; Gani, R., Kontogeorgis, G. K., Eds.; Elsevier: Amsterdam, 2004.

(2) Leahy-Dios, A.; Firoozabadi, A. Molecular and Thermal Diffusion Coefficients of Alkane-Alkane and Alkane-Aromatic Binary Mixtures: Effect of Shape and Size of Molecules. *J. Phys. Chem. B* **2007**, *111*, 191−198.

(3) Alonso De Mezquia, D.; Bou-Ali, M. M.; Larrañaga, M.; Madariaga, J. A.; Santamaría, C. Determination of Molecular Diffusion Coefficient in n-Alkane Binary Mixtures: Empirical Correlations. *J. Phys. Chem. B* **2012**, *116*, 2814−2819.

(4) Blanco, P.; Polyakov, P.; Bou-Ali, M.; Wiegand, S. Thermal Diffusion and Molecular Diffusion Values for Some Alkane Mixtures: a Comparison between Thermogravitational Column and Thermal Diffusion Forced Rayleigh Scattering. *J. Phys. Chem. B* **2008**, *112*, 8340−8345.

(5) Sundelöf, L. O. Definition and Interpretation of an Apparent Diffusion Coefficient in Multicomponent Systems. *J. Chem. Soc., Faraday Trans. 2* **1981**, *77*, 1779.

(6) Kett, T. K.; Anderson, D. K. Ternary Isothermal Diffusion and the Validity of the Onsager Reciprocal Relations in Non-associating Systems. *J. Phys. Chem.* **1969**, *73*, 1268.

(7) Wesselingh, J. A.; Bollen, A. M. Multicomponent Diffusivities from the Free Volume Theory. *Chem. Eng. Res. Des.* **1997**, *75*, 590.

(8) Galliero, G.; Medvedev, O. O.; Shapiro, A. A. Molecular Dynamics Simulations of the Penetration Lengths: Application within the Fluctuation Theory for Diffusion Coefficients. *Phys. A* **2005**, *350*, 315−337.

(9) Liu, X.; Schnell, S. K.; Simon, J. M.; Krüger, P.; Bedeaux, D.; Kjelstrup, S.; Bardow, A.; Vlugt, T. J. H. Diffusion Coefficients from Molecular Dynamics Simulations in Binary and Ternary Mixtures. *Int. J. Thermophys.* **2013**, *34*, 1169−1196.

(10) Pařez, S.; Guevara-Carrion, G.; Hasse, H.; Vrabec, J. Mutual Diffusion in the Ternary Mixture of Water + Methanol + Ethanol and its Binary Subsystems. *Phys. Chem. Chem. Phys.* **2013**, *15*, 3985.

(11) Mialdun, A.; Sechenyh, V.; Legros, J. C.; Ortiz de Zárate, J. M.; Shevtsova, V. Investigation of Fickian Diffusion in the Ternary Mixture of 1, 2, 3, 4-Tetrahydronaphthalene, Isobutylbenzene, and Dodecane. *J. Chem. Phys.* **2013**, *139*, 104903.

(12) Sechenyh, V.; Legros, J. C.; Shevtsova, V. Development and Validation of a New Setup for Measurements of Diffusion Coefficients in Ternary Mixtures Using the Taylor Dispersion Technique. *C. R. Mec.* **2013**, *341*, 490−496.

(13) Larrañaga, M.; Bou-Ali, M. M.; Lizarraga, I.; Madariaga, J. A.; Santamaría, C. Soret Coefficients of the Ternary Mixture 1, 2, 3, 4-Tetrahydronaphthalene + Isobutylbenzene + n-Dodecane. *J. Chem. Phys.* **2015**, *143*, 024202.

(14) Königer, A.; Wunderlich, H.; Köhler, W. Measurement of Diffusion and Thermal Diffusion in Ternary Fluid Mixtures Using a Two-color Optical Beam Deflection Technique. *J. Chem. Phys.* **2010**, *132*, 174506.

(15) Mialdun, A.; Yasnou, V.; Shevtsova, V. Measurement of Isothermal Diffusion Coefficients in Ternary Mixtures Using Counter Flow Diffusion Cell. *C. R. Mec.* **2013**, *341*, 462−468.

(16) Riede, T. H.; Schluder, E. U. Diffusivities of the Ternary Liquid Mixture 2-Propanol-Water-Glycerol and Three-component Mass Transfer in Liquids. *Chem. Eng. Sci.* **1991**, *46*, 609−617.

(17) Grossmann, T.; Winkelmann, J. Ternary Diffusion Coefficients of Glycerol + Acetone + Water by Taylor Dispersion Measurements at 298.15 K. *J. Chem. Eng. Data* **2005**, *50*, 1396−1403.

(18) Grossmann, T.; Winkelmann, J. Ternary Diffusion Coefficients of Cyclohexane + Toluene + Methanol by Taylor Dispersion Measurements at 298.15 K. Part 2. Low Toluene Area Near the Binodal Curve. *J. Chem. Eng. Data* **2009**, *54*, 485−490.

(19) Rehfeldt, S.; Stichlmair, J. Measurement and Prediction of Multicomponent Diffusion Coefficients in Four Ternary Liquid Systems. *Fluid Phase Equilib.* **2010**, *290*, 1−14.

(20) Ray, G. B.; Leaist, D. G. Measurement of Ternary Mutual Diffusion Coefficients from Ill-Conditioned Taylor Dispersion Profiles in Cases of Identical or Nearly Identical Eigenvalues of the Diffusion Coefficient Matrix. *J. Chem. Eng. Data* **2010**, *55*, 1814−1820.

(21) Legros, J. C.; Gaponenko, Y.; Mialdun, A.; Triller, T.; Hammon, A.; Bauer, C.; Köhler, W.; Shevtsova, V. Investigation of Fickian Diffusion in the Ternary Mixtures of Water-Ethanol-Triethylene Glycol and its Binary Pairs. *Phys. Chem. Chem. Phys.* **2015**, *17*, 27713−27725.

(22) Wambui Mutoru, J. W.; Firoozabadi, A. Form of Multicomponent Fickian Diffusion Coefficients Matrix. *J. Chem. Thermodyn.* **2011**, *43*, 1192−1203.

(23) Price, W. E. Theory of the Taylor Dispersion Technique for Three-component-system Diffusion Measurements. *J. Chem. Soc., Faraday Trans. 1* **1988**, *84*, 2431−2439.

(24) Shevtsova, V.; Gaponenko, Y. A.; Sechenyh, V.; Melnikov, D. E.; Lyubimova, T.; Mialdun, A. Dynamics of a Binary Mixture Subjected to a Temperature Gradient and Oscillatory Forcing. *J. Fluid Mech.* **2015**, *767*, 290.

(25) Mialdun, A.; Legros, J. C.; Yasnou, V.; Sechenyh, V.; Shevtsova, V. Contribution to the Benchmark for Ternary Mixtures: Measurement of the Soret, Diffusion and Thermodiffusion Coefficients in the Ternary Mixture THN/IBB/nC12 with 0.8/0.1/0.1 Mass Fractions in Ground and Orbital Laboratories. *Eur. Phys. J. E: Soft Matter Biol. Phys.* **2015**, *38*, 27.

(26) Galand, Q.; Van Vaerenbergh, S. Contribution to the Benchmark for Ternary Mixtures: Measurement of the Soret, Diffusion and Thermodiffusion Coefficients in the Ternary Mixture THN/IBB/nC12 with 0.8/0.1/0.1 Mass Fractions in Ground and Orbital Laboratories. *Eur. Phys. J. E: Soft Matter Biol. Phys.* **2015**, *38*, 26.

(27) Ahadi, A.; Ziad Saghir, M. Contribution to the Benchmark for Ternary Mixtures: Transient Analysis in Microgravity Conditions. *Eur. Phys. J. E: Soft Matter Biol. Phys.* **2015**, *38*, 25.

(28) Khlybov, A.; Ryzhkov, I. I.; Lyubimova, T. P. Contribution to the Benchmark for Ternary Mixtures: Measurement of Diffusion and Soret Coefficients in 1,2,3,4-Tetrahydronaphthalene, Isobutylbenzene, and Dodecane Onboard the ISS. *Eur. Phys. J. E: Soft Matter Biol. Phys.* **2015**, *38*, 29.

(29) Bou-Ali, M. M.; Ahadi, A.; Alonso de Mezquia, D.; Galand, Q.; Gebhardt, M.; Khlybov, O.; Köhler, W.; Larranaga, M.; Legros, J. C.; Lyubimova, T.; et al. Benchmark Values for the Soret, Thermodiffusion and Molecular Diffusion Coefficients of the Ternary Mixture Tetralin+Isobutylbenzene+n-Dodecane with 0.8−0.1−0.1 Mass Fraction. *Eur. Phys. J. E: Soft Matter Biol. Phys.* **2015**, *38*, 30.

(30) Mialdun, A.; Shevtsova, V. Communication: New Approach for Analysis of Thermodiffusion Coefficients in Ternary Mixtures. *J. Chem. Phys.* **2013**, *138*, 161102.

(31) Rutten, W. M. *Diffusion in Liquids*, Ph.D. Dissertation, Delft University: Delft, The Netherlands, 1992.

DOI: 10.1021/acs.jpcb.5b11143
J. Phys. Chem. B 2016, 120, 535−548

(32) Halvorsen, H. M.; Wygnal, E.; MacIver, M. R.; Leaist, D. G. Ternary Mutual Diffusion Coefficients from Error-Function Dispersion Profiles: Aqueous Solutions of Triton X-100 Micelles + Poly(ethylene glycol). *J. Chem. Eng. Data* **2007**, *52*, 442−448.
(33) Alizadeh, A.; Nieto de Castro, C. A. N.; Wakeham, W. A. The theory of the Taylor Dispersion Technique for Liquid Diffusivity Measurements. *Int. J. Thermophys.* **1980**, *1*, 243.
(34) Taylor, G. I. Conditions Under which Dispersion of a Solute in a Stream of Solvent can be Used to Measure Molecular Diffusion. *Proc. R. Soc. London, Ser. A* **1954**, *225*, 473−477.
(35) Leaist, D. G. Ternary Diffusion Coefficients of 18-Crown-6 Ether-KCI-Water by Direct Least-squares Analysis of Taylor Dispersion Measurements. *J. Chem. Soc., Faraday Trans.* **1991**, *87* (4), 597−601.
(36) Wakeham, W. A.; Nagashima, A.; Sengers, J. V., Eds. *Measurement of the Transport Properties of Fluids*; Blackwell: London, 1991.
(37) Deng, Z.; Leaist, D. G. Ternary Mutual Diffusion Coefficients of MgCl2 + MgSO4 + H2O and Na2SO4 + MgSO4 + H2O from Taylor Dispersion Profiles. *Can. J. Chem.* **1991**, *69*, 1548−1553.
(38) Taylor, R.; Krishna, R. *Multicomponent mass transfer*. Wiley: New York, 1993.
(39) Sechenyh, V.; Legros, J. C.; Shevtsova, V. Optical Properties of Binary and Ternary Liquid Mixtures Containing Tetralin, Isobutylbenzene and Dodecane. *J. Chem. Thermodyn.* **2013**, *62*, 64−68.
(40) Gill, P. E.; Murray, W.; Saunders, M. A.; Wright, M. H. Procedures for Optimization Problems with a Mixture of Bounds and General Linear Constraints. *ACM Trans. Math. Software* **1984**, *10*, 282−298.
(41) Gebhardt, M.; Köhler, W. What Can be Learned from Optical Two-color Diffusion and Thermodiffusion experiments on ternary fluid mixtures? *J. Chem. Phys.* **2015**, *142*, 084506.
(42) Gupta, P. K., Jr.; Cooper, A. R. The [D] Matrix for Multicomponent Diffusion. *Physica* **1971**, *54* (1), 39−59.
(43) Thompson, M. S.; Morral, J. E. The Effect of Composition on Interdiffusion in Ternary alloys. *Acta Metall.* **1986**, *34*, 339−346.
(44) Gebhardt, M.; Köhler, W.; Mialdun, A.; Yasnou, V.; Shevtsova, V. Diffusion, Thermal Diffusion, and Soret Coefficients and Optical Contrast Factors of the Binary Mixtures of Dodecane, Isobutylbenzene, and 1,2,3,4-Tetrahydronaphthalene. *J. Chem. Phys.* **2013**, *138*, 114503.

DOI: 10.1021/acs.jpcb.5b11143
J. Phys. Chem. B 2016, 120, 535−548